Sound & Vibration 2026, 60(1), 3813.
doi: https://doi.org/10.59400/sv3813

Article

An investigation on the friction-induced vibration in train brake blocks on slack adjuster compensator

Nutthapong Kunla[1], Anan Suebsomran[2,*]

[1] Department of Mechanical Engineering, Faculty of Engineering, Bangkokthonburi University, 16/10 Thawi Watthana Road, Thawi Watthana, Bangkok 10170, Thailand

[2] Department of Teacher Training in Mechanical Engineering, Faculty of Technical Education, King Mongkut's University of Technology North Bangkok, 1518 Pracharat 1 Road, Bangsue, Bangkok 10800, Thailand

*** Corresponding author:** Anan Suebsomran, anan.s@fte.kmutnb.ac.th or asr@kmutnb.ac.th

CITATION

Kunla N, Suebsomran A. An investigation on the friction-induced vibration in train brake blocks on slack adjuster compensator. Sound & Vibration. 2026; 60(1): 3813. https://doi.org/10.59400/sv3813

ARTICLE INFO

Received: 7 December 2025
Revised: 30 December 2025
Accepted: 13 February 2026
Available online: 24 February 2026

Abstract: Friction-induced vibration is a critical issue in railway tread brake systems, as it can affect braking stability, wear, and the dynamic response of mechanically connected components. This study numerically investigates the self-excited vibration behavior of a tread brake unit and its interaction with a slack adjuster compensator under braking conditions. A simplified single-degree-of-freedom dynamic model incorporating a velocity-dependent Coulomb friction formulation is developed to analyze the vibration response of the brake block under continuous sliding conditions. The governing nonlinear differential equation is solved using the Runge–Kutta method, and time- and frequency-domain analyses are performed to identify dominant vibration characteristics. The numerical results indicate the presence of low-frequency self-excited vibration induced by dry friction, while the contact interface remains in a continuous sliding regime and no classical stick–slip transition involving intermittent adhesion is observed. The dominant vibration frequency is approximately 0.35 Hz, reflecting the global mass–stiffness dynamics of the brake unit rather than high-frequency stick–slip or squeal phenomena. A finite element modal analysis of the slack adjuster compensator shows that its natural frequencies are several orders of magnitude higher than the dominant vibration frequency, indicating that resonance is unlikely under the investigated operating conditions. The findings provide insight into friction-induced vibration mechanisms in railway tread brake systems and their implications for vibration safety and structural integrity.

Keywords: friction-induced vibration; railway tread brake; self-excited vibration; Coulomb friction model; slack adjuster compensator

1. Introduction

Railway braking systems constitute a vital safety subsystem, as they are responsible for dissipating the kinetic energy of a moving vehicle through friction at the wheel tread–brake block interface. In conventional railway air braking systems, brake blocks are applied directly to the wheel tread via a mechanically coupled brake rigging that typically includes slack adjusters and compensator mechanisms. During braking, this interconnected structure is subjected not only to static braking forces but also to dynamic loads, which may induce vibration and contribute to the degradation of mechanically connected components.

Friction-induced vibration is a well-documented phenomenon in mechanical systems involving sliding or rolling contact and has been widely investigated within

the framework of nonlinear dynamics [1–3]. Previous studies have demonstrated that frictional interfaces may act as an energy source, leading to self-excited oscillations when coupled with compliant structural elements [2]. In railway applications, frictional contact behavior is inherently nonlinear and governed by strong interactions between contact mechanics and structural dynamics. Dynamic friction models have further shown that the friction coefficient cannot be treated as a constant during braking, but instead varies with sliding velocity, normal load, surface condition, and thermal effects [4]. Such variations play an essential role in the initiation and evolution of friction-induced vibration.

The variability of friction and its dynamic consequences in railway systems have been examined in several studies. Meacci et al. [5] proposed a local degraded adhesion model for wheel–rail contact and showed that significant sliding and energy dissipation can result in pronounced time-dependent frictional behavior during braking. Yang et al. [6, 7] further demonstrated that dynamic frictional interactions at contact interfaces may trigger complex vibration responses due to coupling between friction forces and structural motion. Experimental work by Ostermeyer and Wilkening [8] revealed that friction coefficients in brake pads evolve over time owing to the generation and destruction of contact patches within the boundary layer, emphasizing the history-dependent and dynamic nature of friction under braking conditions.

A large proportion of existing research on friction-induced vibration has focused on disc brake systems, particularly with regard to brake squeal, creep–groan, and stick–slip instabilities. Lu et al. [9] and Wang et al. [10] investigated stick–slip vibration mechanisms in disc–block configurations, while Crowther and Singh [11,12] showed that discontinuous friction forces associated with stick–slip transitions can excite significant vibration responses in coupled brake–driveline systems. More recent nonlinear dynamic studies have reported that braking speed, contact pressure, and structural coupling may lead to bifurcation phenomena, chaotic behavior, and low-frequency self-excited vibration under low-speed braking conditions [13, 14]. Despite their contributions, these studies primarily address disc brake systems or vibration mechanisms dominated by stick–slip behavior, which differ fundamentally from the continuous sliding conditions examined in the present work.

In contrast, friction-induced vibration in railway tread brake systems has received comparatively limited attention. Previous investigations have indicated that the braking performance and frictional characteristics of tread brakes are strongly influenced by operating and environmental factors. Zhang et al. [15] demonstrated that surface ice can significantly reduce friction levels and impair braking effectiveness, while Günay et al. [16] discussed the operational characteristics and widespread application of tread brake systems in railway vehicles. Mickoski et al. [17] reported that dry friction in tread brake units may lead to sustained oscillations under certain conditions. However, most existing studies consider the brake block as an isolated component and do not explicitly address the dynamic interaction with mechanically coupled brake rigging elements.

Friction-induced vibration in mechanically coupled systems has also been examined in the context of automotive and braking dynamics. Duan and Singh [18] showed that dry friction in multi-degree-of-freedom systems may act as a destabilizing

mechanism analogous to negative damping, while Shin et al. [19] demonstrated that modal coupling in the presence of friction can give rise to self-excited vibration when interacting modes are closely spaced. Although these investigations focused primarily on disc brake configurations, the underlying principles of friction-induced excitation and modal interaction are also relevant to railway tread brake systems with mechanically interconnected brake rigging.

From a vibration and resonance standpoint, it is well established that substantial response amplification may occur when excitation frequencies approach the natural frequencies of interacting structural components, whereas sufficient frequency separation generally results in non-resonant behavior [20]. In practical railway air braking systems, frictional excitation generated at the wheel tread–brake block interface is transmitted through a dynamically coupled structure comprising the brake block, brake rigging, and slack adjuster. Experimental studies have shown that braking torque and frictional forces can significantly influence the dynamic response of railway vehicle subsystems [21, 22], indicating that friction-induced vibration may propagate beyond the local contact interface and affect mechanically connected components.

The air brake, as shown in **Figure 1**, is a widely used fail-safe braking system in railway vehicles, in which compressed air is employed to actuate the brake rigging and apply braking force at the wheel tread.

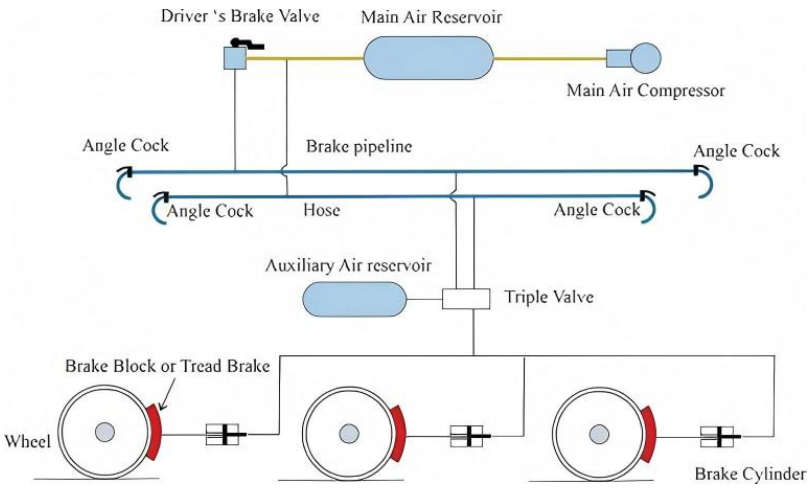

Figure 1. Main parts of the air braking system.

The slack adjuster is a critical mechanical component of railway air braking systems, responsible for maintaining an appropriate clearance between the brake blocks and the wheel tread as wear progresses, thereby ensuring consistent braking performance. In tread brake configurations, the slack adjuster and its compensator are mechanically integrated into the brake rigging and directly transmit braking forces from the brake cylinder to the brake blocks, pressing them against the wheel tread. The compensator, typically implemented as a slender threaded rod, is therefore subjected not only to static braking loads but also to dynamic forces and vibration during braking. Friction-induced vibration generated at the wheel–brake block interface may propagate through the brake rigging and excite the slack adjuster compensator. Under unfavorable dynamic conditions, such excitation may result in excessive vibration, deformation, or even structural damage, as illustrated in **Figure 2**, particularly if resonance occurs

between the excitation frequencies and the natural frequencies of the compensator.

Figure 2. Bent tread compensator of the air braking system [17].

For the air braking system used in the GEA 4523–4560 series freight locomotives operated in Thailand, the resonance characteristics of the slack adjuster compensator have not yet been verified through numerical or experimental investigations. Moreover, the service lifetime of the compensator cannot be reliably estimated based solely on tread material properties or static design considerations.

The braking process of railway vehicles is governed by multiple interacting factors, including braking force generation, frictional characteristics at the contact interface, and wheel–rail adhesion conditions. Mickoski et al. [23] developed a mathematical model for railway vehicle tread braking and demonstrated that both frictional forces and braking resistance exhibit nonlinear and time-varying behavior throughout the braking process. Their experimental investigations further revealed that brake blocks experience measurable vibration during the entire braking interval, even under nominal operating conditions. However, the implications of such vibration on mechanically coupled brake rigging components have not been fully addressed.

Despite the extensive literature on friction-induced vibration, the dynamic interaction between tread brake-induced vibration and slack adjuster compensators has not yet been systematically investigated. In particular, it remains unclear whether friction-induced self-excited vibration under continuous sliding conditions can excite the compensator and lead to resonance or adverse dynamic behavior in practical railway air braking systems.

Accordingly, the present study numerically investigates friction-induced self-excited vibration in a railway tread brake system operating under continuous sliding conditions, with particular emphasis on its interaction with a slack adjuster compensator. A simplified single-degree-of-freedom dynamic model incorporating a velocity-dependent Coulomb friction formulation is employed to analyze the vibration response of the brake block. The dominant vibration frequencies are subsequently compared with the natural frequencies of the slack adjuster compensator obtained from finite element modal analysis to assess the likelihood of resonance under representative braking conditions. The results provide further insight into friction-induced vibration mechanisms in tread brake systems and support a resonance-based evaluation of vibration safety in mechanically coupled brake components.

The rest of this paper is structured as follows. Section 2 describes the methodology of our scheme. Section 3 describes the characteristics of the tread braking system. Section 4 describes the modeling of friction-induced vibration. Section 5 describes the Coulomb friction model. Section 6 analyzes the friction-induced vibration of the braking unit system. Section 7 reports the results of the modal analysis of the slack adjuster compensator. Section 8 is a discussion. Section 9 concludes the paper and

describes the future work.

2. Methodology

The analysis method for the vibrational behavior study of the brake tread was numerical simulation utilizing a nonlinear differential equation of the nonlinear friction force. The orientation of the brake tread and its vibration with respect to the relative velocity. The response of the nonlinear dynamical system corresponding to the initial condition was calculated numerically using the Runge-Kutta integration method included in MATLAB software through the ODE45 function and the Fast Fourier transform was used to calculate the frequencies of self-excited vibration of the brake tread. A Finite Element Method (FEM) program. FEM was used to analyze the natural frequency of the tread in the air braking system. A flowchart diagram illustrating the procedures in this methodology is in **Figure 3**.

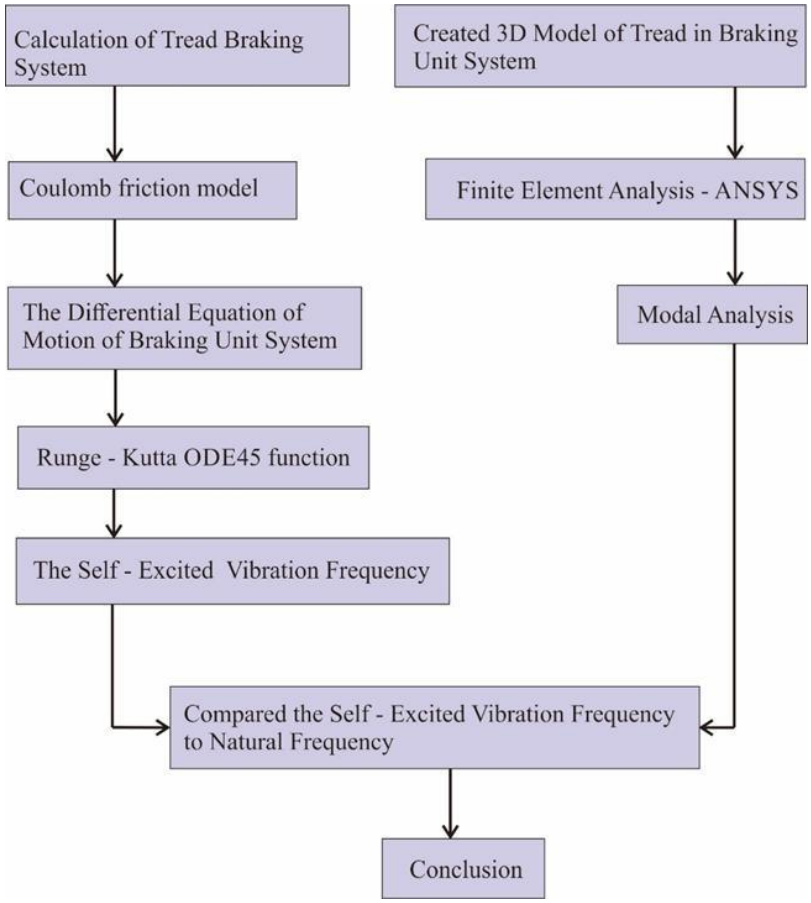

Figure 3. The flowchart illustrates the methodology of the paper.

3. Characteristics of the tread braking system

The permissible train velocity is confined to its ability to stop at a safe distance in case of an emergency. The stopping distance is determined by the ratio of the total braking force developed by the brake shoes and the mass of the train.

The braking forces are mostly determined by the friction coefficients. Numerous factors, including running speed, clamping force, and contact surface pressure, affect these coefficients. A vehicle's immediate running speed, contact pressure, and applied

force on each shoe all have significant impacts on the coefficient of friction between the brake shoe and wheel tread.

Figure 4 includes photos of the GE-produced GE CM22-7i diesel-electric locomotive in Southeast Asia. These days, the locomotive is operated by the State Railway of Thailand under the code series number GEA 4523–4560. The bogie brake rigging of a 14.42-t axle load bogie is as shown in **Figure 5**.

(a) **(b)**

Figure 4. The diesel-electric locomotive series GEA 4523–4560 used in the paper **(a)** The diesel-electric locomotive series GEA 4523 for passenger and freight traffic [24]; **(b)** The diesel-electric locomotive series GEA 4558 for passenger and freight traffic [25].

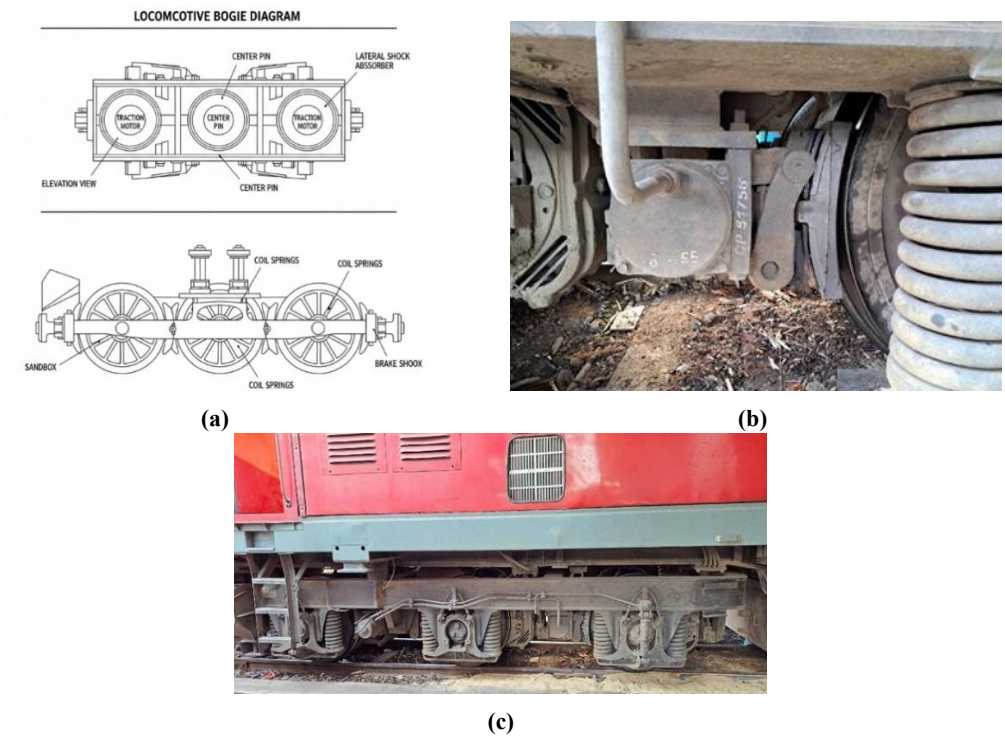

(a) **(b)**

(c)

Figure 5. **(a)** Drawing of the bogie brake rigging of a 14.42-t axle load bogie; **(b)** Drum Brake Assembly on Bogie Brake Rigging of GE CM22-7i Locomotive; **(c)** The bogie brake rigging of a 14.42-ton axle load bogie.

Table 1 provides an overview of the specifications for the GEA 4523–4560 series of diesel-electric locomotives. The specifications of the traction brake are detailed in **Table 2**.

Table 1. Specifications of locomotive (GE CM22-7i or GEA 4523–4560).

Technical category	Symbol	Unit	Value
Total vehicle weight	w	kg	86,500
The speed at which the braking starts	*v*	km/h	40
Overall height of the vehicle	H	mm	3635
Overall length of the vehicle	L	mm	19,355
Overall width of vehicle	W	mm	2820
Wheel diameter with tire	Dw	mm	914
Coefficient of dry friction	μ		0.3

Table 2. Specifications of the air brake system.

Technical category	Symbol	Value
Brake cylinder diameter	D_c	203 mm
Maximum brake cylinder	P	0.38 N/mm^2
Leverage ratio	r_L	366:174
No. of levers per axle	n_L	2
No. of brake blocks	N_b	24
Brake cylinder efficiency	η_c	0.9
Rigging efficiency	η_r	0.9
Coefficient of friction between the brake block and the wheel	μ	0.3
Brake block width	B	79.4 mm

Brake force calculation

The air brake system data provided in **Table 2** is used in Equations (1)–(7) to compute the braking force on the air brake system.

— Area of the piston, (Ap)

$$A_P = \pi r_r^2 \tag{1}$$

— Force available on the piston

$$F_P = A_P \times P \tag{2}$$

— Mechanical advantage/axle

$$MA = r_L \times n_L \tag{3}$$

— Theoretical braking force available on an axle

$$(F_a)_{theo} = F_P \times MA \tag{4}$$

— Theoretical braking force available on a coach

$$(F_c)_{theo} = (F_a)_{theo} \times 12 \tag{5}$$

— Theoretical braking force on each brake block

$$(F_b)_{theo} = \frac{(F_c)_{theo}}{24} \tag{6}$$

— Actual braking force available on each brake block

$$(F_b)_{actual} = (F_b)_{theo} \times \eta_c \times \eta_r \tag{7}$$

Table 3 shows the calculated values of the braking force in the air brake system, which is uniformly applied to all wheels.

Table 3. Brake force calculated values.

Description	Symbol	Unit	Value
Brake block curve length		mm	317.5
Brake block area		mm	25210
Pressure	P	N/mm^2	0.38
Theoretical braking force available on each brake block	$(F_b)_{theo}$	kN	12.92
Actual brake force available on each brake block	$(F_b)_{actual}$	kN	10.46
Area of the piston	A	mm^2	32349
Piston force	F_P	kN	12.3
Mechanical advantage/axle	MA		4.2
Theoretical braking force available on an axle	F_a	kN	51.66

The forces acting on the wheels under a level condition are shown in **Figure 6**. The assumption was that the friction coefficient between the wheel and the brake block remains constant, with an average value determined by the design of the brake tread.

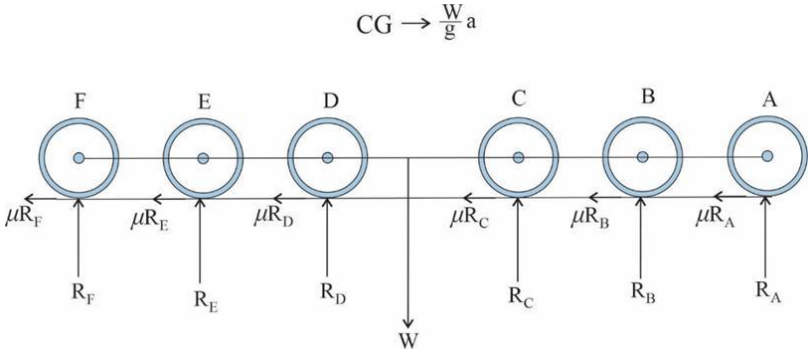

Figure 6. Forces acting on the wheels of a vehicle under level-track conditions.

Using the braking force calculated in **Table 3** together with the total vehicle mass listed in **Table 1**, the deceleration, stopping distance, and braking time were obtained based on classical kinematic relationships under level-track conditions. The resulting braking performance parameters are summarized in **Table 4**.

Table 4. Results on a moving vehicle.

Description	Unit	Value
Deceleration	m/s^2	3.924
Stopping Distance	m	15.73
Braking Time	s	2.832
Efficiency	%	40

The speed at which the train started to brake was 40 km/h. The brake force created by the brake unit was 10.46 kN.

4. Modeling of friction-induced vibration

The phenomenon of stick-slip occurs when surfaces alternate between sliding over one another and adhering to one another, resulting in a corresponding variation in the frictional force. In general, the coefficient of static friction between the two surfaces is greater in magnitude than the coefficient of kinetic friction. When the magnitude of the applied force surpasses the static friction, the transition from friction to kinetic friction can result in an abrupt increase in the velocity of the object in motion. By considering only pad elasticity in one direction, this effect can be illustrated as a simplified representation of the frictional coupling between the brake block and disc, which is represented by a dynamic model with at least one degree of freedom (DOF) (**Figure 7**), to facilitate the theoretical investigation of self-excited vibrations.

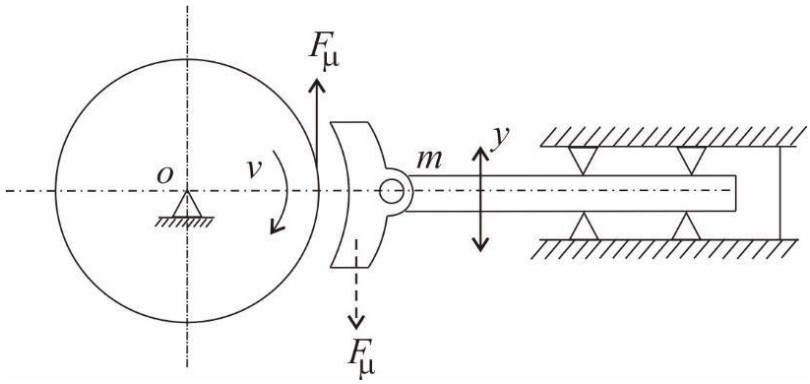

Figure 7. Dynamical Model of the Tread of the Brake [17].

The purpose of the present model is not to reproduce a full stick–slip transition, but to examine whether friction-induced vibration under typical braking conditions can excite the slack adjuster compensator.

4.1. Dynamic model of the tread brake unit

To analyze friction-induced vibration in the tread brake system, a simplified dynamic model of the brake unit is adopted based on the formulation proposed by Mickoski et al. [17]. The model considers the vibration of the brake block relative to the wheel tread and captures the essential features of frictional coupling responsible for self-excited vibration. A single-degree-of-freedom representation is employed, as illustrated in **Figure 7**, where the brake block is modeled as a mass–spring system subjected to a nonlinear friction force at the wheel–brake block interface.

The governing differential equation of the model is:

$$m\ddot{y}(t) + c\dot{y}(t) + ky(t) = F_u(v_{rel}) \tag{8}$$

The nonlinear friction force varies in direction and value in relation to relative velocity. Equation (8) is a nonlinear differential equation.

The response of the nonlinear dynamical system corresponding to the initial condition was calculated numerically using the Runge-Kutta integration method included in MATLAB software through the ODE45 function.

where

m is the equivalent mass of the brake block,

c is the damping coefficient,

k is the stiffness of the brake block mounting, and

F_u is the nonlinear friction force.

y is the relative displacement of the brake block, and

v_{rel} is the relative sliding velocity between the brake block and the wheel tread.

4.2. Relative sliding velocity and operating conditions

In the present analysis, friction-induced vibration is examined with respect to the relative sliding motion between the brake block and the wheel tread, rather than assuming an idealized pad–disc configuration. During braking, the wheel tread velocity decreases according to a prescribed deceleration profile, while the brake block undergoes vibration due to frictional interaction and structural compliance within the brake rigging.

For numerical stability and modeling simplicity, the wheel tread velocity is treated as a slowly varying, prescribed input rather than a dynamic degree of freedom. This assumption is justified by the fact that the wheel tread motion is governed by the global braking dynamics of the vehicle, whereas the vibration amplitude of the brake block is comparatively small. Consequently, the dynamic response of the brake block is evaluated relative to the wheel tread motion.

Under these operating conditions, the contact interface between the brake block and the wheel tread remains in a continuous sliding regime. No sustained adhesion phase is introduced in the formulation, and classical stick–slip transitions are not explicitly modeled. The adopted approach is therefore suitable for investigating friction-induced self-excited vibration under sliding conditions and for identifying dominant vibration frequencies relevant to resonance assessment, rather than for reproducing intermittent stick–slip behavior.

4.3. Friction model and numerical solution

The friction force acting at the wheel tread–brake block interface is modeled using a Coulomb-type dry friction formulation, in which the friction coefficient varies with the relative sliding velocity. The friction force is expressed as:

$$F_u = \mu(v_{rel}) N sgn(v_{rel}) \tag{9}$$

where

$\mu(v_{rel})$ is the velocity-dependent friction coefficient,

N is the normal force acting on the brake block,

$sgn(\cdot)$ is the sign function.

This formulation represents dry sliding friction at the contact interface and does not explicitly model adhesion or sticking behavior. The velocity dependence of the friction coefficient reflects experimentally observed friction characteristics of cast-iron and composite brake shoes under dry contact conditions. In the present study, this dependence is introduced as an excitation mechanism for friction-induced vibration

under continuous sliding conditions, rather than as a detailed interface-resolved friction law.

The resulting nonlinear differential equation of motion is solved numerically using the Runge–Kutta integration scheme implemented in MATLAB via the ODE45 solver. Zero initial displacement and velocity conditions are assumed at the onset of braking. The time-domain response of the brake block velocity is subsequently analyzed using the Fast Fourier Transform (FFT) to extract the dominant frequency components of the friction-induced vibration, which are later compared with the natural frequencies of the slack adjuster compensator.

4.4. Interpretation of vibration response

The computed time histories of the brake block velocity exhibit oscillatory behavior throughout the braking process. However, the relative velocity between the brake block and the wheel tread remains continuously nonzero, and no time interval corresponding to sustained adhesion is observed. This behavior indicates that the contact interface operates predominantly in a continuous sliding regime, rather than undergoing alternating stick and slip phases.

An examination of the phase relationship between the brake block velocity response and the prescribed wheel tread motion further supports this observation. A persistent nonzero phase difference is observed between the two signals, which is consistent with friction-induced self-excited vibration under sliding conditions rather than classical stick–slip oscillation characterized by intermittent adhesion.

Accordingly, the vibration response obtained in the present analysis is interpreted as self-excited vibration arising from nonlinear dry friction under continuous sliding conditions. Under the specified operating parameters, no evidence of classical stick–slip instability is identified. This interpretation provides the basis for subsequent frequency-domain analysis and resonance assessment of the slack adjuster compensator.

4.5. Frequency-domain characteristics

The frequency-domain characteristics of the friction-induced vibration are analyzed using the Fast Fourier Transform (FFT) applied to the time-domain response of the brake block velocity. The FFT analysis is performed to identify the dominant frequency components of the vibration signal during the braking process, rather than to investigate high-frequency noise or squeal phenomena.

The FFT analysis was performed on the brake block velocity signal over the braking interval of 0–2.832 s using a single-sided amplitude spectrum. A uniform time step corresponding to the numerical integration output was adopted, resulting in a frequency resolution sufficient to identify the dominant low-frequency vibration components.

The results reveal a dominant low-frequency component in the vibration response of the brake unit. This frequency is associated with the global dynamic behavior of the brake block system under nonlinear dry friction excitation and continuous sliding conditions. Owing to the relatively large mass and compliance of the brake unit,

the resulting self-excited vibration occurs at a low-frequency scale, distinct from the high-frequency oscillations typically associated with classical stick–slip or brake squeal involving intermittent adhesion.

The identified dominant frequency components are subsequently compared with the natural frequencies of the slack adjuster compensator obtained from finite element modal analysis. This comparison provides the basis for assessing the potential for resonance between the friction-induced vibration of the brake block and the structural dynamics of the compensator, as discussed in the following sections.

5. Coulomb friction model

Dry friction plays a central role in the generation of friction-induced vibration in braking systems. In the present study, a Coulomb-type friction model is adopted to represent the interaction between the brake block and the wheel tread under dry contact conditions. This model provides a simplified and widely accepted description of frictional behavior at low to moderate sliding velocities and is therefore suitable for investigating friction-induced vibration phenomena in braking systems.

It is important to emphasize that, in this formulation, the friction model is employed to analyze friction-induced vibration under sliding-dominated operating conditions rather than to explicitly simulate a complete stick–slip transition. The adopted model implicitly assumes continuous sliding at the wheel tread–brake block interface and does not incorporate a distinct sticking phase. This modeling assumption is consistent with the numerical responses obtained in the present study and with the objective of identifying dominant vibration characteristics relevant to resonance assessment, as discussed in the following sections.

5.1. Friction force formulation

The friction force acting at the wheel tread–brake block interface is expressed as:

$$F_u = \mu N sgn(v_{rel}) \tag{10}$$

where

F_u is the force of friction;

μ is the coefficient of friction;

N is the normal force pressing the surfaces together;

v_{rel} is the relative sliding speed between the wheel tread and the brake block.

In the present analysis, the relative sliding velocity is approximated by the wheel tread velocity during braking. This represents an engineering approximation adopted under the assumption of continuous sliding and relatively small vibration amplitudes of the brake block compared with the wheel tread motion. Under these conditions, the wheel tread velocity provides an effective representation of the sliding state at the contact interface.

Accordingly, the friction coefficient is expressed as a function of the wheel tread velocity. This formulation is not intended to represent a detailed interface-resolved friction law, but rather to capture the dominant velocity-dependent characteristics

of dry friction and to provide a physically consistent excitation mechanism for friction-induced vibration analysis.

5.2. Velocity-dependent friction coefficient

Experimental observations reported in the literature indicate that the coefficient of friction of brake blocks varies with sliding velocity, particularly at low speeds. This velocity dependence introduces nonlinearity into the friction force and may act as a source of friction-induced self-excited vibration. In the present study, the friction coefficient–velocity relationships for cast-iron and composite brake shoes are adopted from the experimental data reported by Ivanov et al. [26], which provide representative trends of dry friction behavior under railway braking conditions.

$$\mu = f(\nu) \tag{11}$$

where v is the wheel tread velocity during braking.

In the present formulation, the wheel tread velocity is used as an engineering approximation of the relative sliding velocity at the wheel tread–brake block interface. This approximation is considered reasonable under the assumed operating conditions of continuous sliding and relatively small vibration amplitudes of the brake block compared with the wheel tread motion.

The velocity profile is prescribed based on the braking deceleration from the initial train speed of 40 km/h to a full stop. The corresponding friction coefficient curves for cast-iron and composite brake shoes under the specified normal load are shown in **Figure 8**. These friction–velocity characteristics illustrate the nonlinear nature of dry friction and its potential to induce self-excited vibration under sliding conditions. However, the presence of a velocity-dependent friction coefficient alone does not necessarily imply the occurrence of stick–slip vibration, which additionally requires intermittent adhesion at the contact interface.

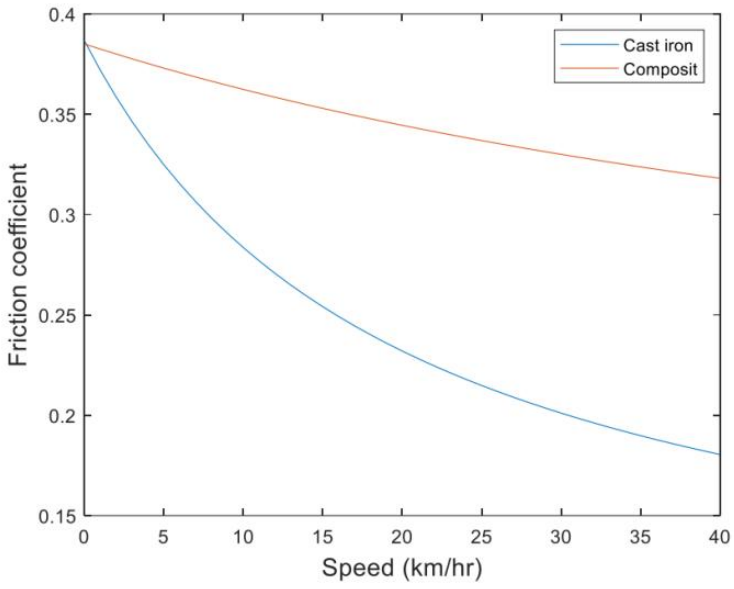

Figure 8. Dependence of friction coefficient on train velocity for the cast-iron brake shoe at pressure force = 9.5147 kN.

For the numerical implementation, the relative sliding velocity is formally defined as:

$$v_{rel} = \nu_1 - \dot{y} \tag{12}$$

Where $\dot{y}$ is the tangential speed of the block, and v_1 is the wheel tread which the deceleration started at v_1 = 40 km/h and continued until t = 2.832 s, or until the train approached zero speed. Approximately, the decreasing velocity of the train is described by Equation (13):

$$\nu_1[\text{m/s}] = 11.11 - 3.92\text{*t} \tag{13}$$

and $sgn(v_{rel})$ is a sign function given by,

$$sgn(\dot{\text{y}} - \nu) \begin{cases} -1 \text{ if } \nu_{rel} < 0 \\ 0 \text{ if } \nu_{rel} = 0 \\ 1 \text{ if } \nu_{rel} > 0 \end{cases} \tag{14}$$

where

$$\nu_{rel} = \begin{cases} \nu, \ \dot{\text{y}} = 0 formal\ definition\ only \\ 0, \ \dot{\text{y}} = \nu formal\ definition\ only \end{cases} \tag{15}$$

Although this formal definition is included for completeness, the numerical response remains entirely within the sliding regime under the investigated operating conditions.

For cast-iron brake shoes and composite brake shoes, the coefficient of friction was determined by an experimental method. The relationship between the friction coefficient and velocity, as indicated in the work of Ivanov et al. [26], is given in km/h; therefore, to convert Equation (10), which is in the form of m/s, to Equation (16). This form of v_2 can be substituted in Equations (17) and (18), so that the coefficient of friction of cast-iron brake shoes and composite brake shoes under pressure force 9.5147 kN are as shown in **Figure 8**.

$$v_2 \text{ [km/h]} = 40 - 14.126\text{*t} \tag{15}$$

$$\mu_c = 0.6 \cdot \frac{1.6T + 100}{8T + 100} \cdot \frac{v_2 + 100}{5v_2 + 100} \tag{16}$$

$$\mu_{com} = 0.44 \cdot \frac{0.1T + 20}{0.4T + 20} \cdot \frac{v_2 + 150}{2v_2 + 150} \tag{17}$$

μ_c = The coefficient of friction between the wheel tread and cast-iron brake shoe

μ_{com} = The coefficient of friction between the wheel tread and composite brake shoe

T = brake force (kN)

v_2 = Train velocity (km/h)

5.3. Implications for vibration analysis

The adopted Coulomb-type friction model introduces nonlinearity into the governing equation of motion of the brake block and acts as the excitation mechanism for friction-induced vibration under sliding conditions. Within the assumed operating parameters and modeling formulation, the friction force varies continuously with the prescribed relative velocity, resulting in an oscillatory response of the brake block that is consistent with continuous sliding behavior. Under these conditions, no sustained sticking phase is observed in the numerical response.

Accordingly, the subsequent vibration analysis focuses on evaluating the dynamic response of the brake block under sliding-dominated conditions and on identifying the dominant frequency components associated with friction-induced self-excited vibration. These frequency components are then compared with the natural frequencies of the slack adjuster compensator to assess the likelihood of resonance under the specified operating conditions, as discussed in the following sections.

6. Analysis of friction-induced vibration of the braking unit system

The bolt's stiffness for fastening the brake tread to the pivot point and the mass of the braking unit system are provided in **Table 5**.

Table 5. Parameters of brake tread model.

Parameter	Unit	Value
Mass	kg	1.3177
Young's Modulus	GPa	200
Moment of inertia	m^4	$2.97181698 \times 10^{-8}$
Stiffness	N/m	6.6040×10^5

$$\nu\ [\mathrm{m/s}] = 11.11 - 3.92\mathrm{*t} \tag{18}$$

The dynamic analysis of the braking unit system, when the train decelerated from a speed of 40 km/h to a full stop, is defined by Equation (19), which is the dynamic model of the brake unit (**Figure 7**) established by Mickoski et al. [17].

The differential equation solution during braking provides the time-domain reaction of the brake block. The diagrams in **Figures 9** and **10** illustrate the velocities of the composite pad brake block and the cast iron pad brake block as the train decelerated from 40 km/h to a full stop. These graphics illustrate the vibration pattern and are used to determine the frequency of the self-excited vibrations.

Figures 11 and **12** show that the friction force between the wheel and brake block was nonlinear, and the speed of brake block vibration was out of phase with the wheel's speed, indicating no adhesion. This response indicates the absence of sustained adhesion at the contact interface. The observed behavior is consistent with continuous relative sliding between the brake block and the wheel tread during vibration, and no classical stick–slip transition is identified under the investigated operating conditions [27].

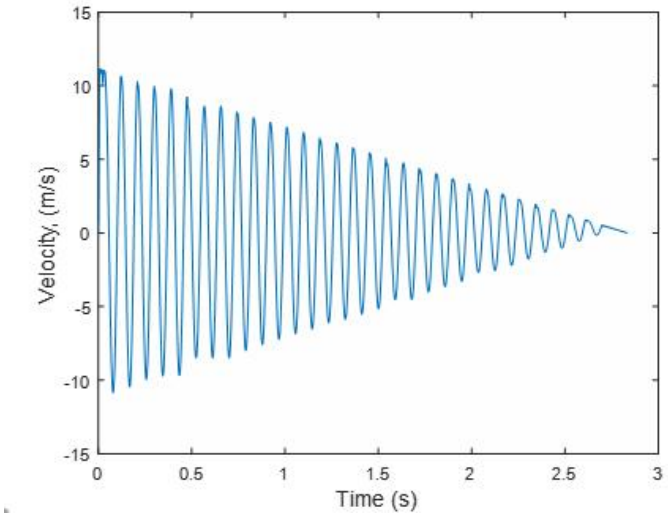

Figure 9. Cast iron pad brake unit vibration during train braking.

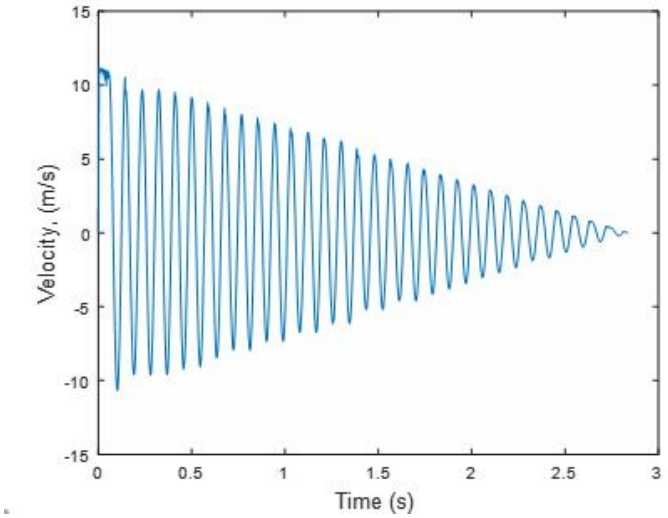

Figure 10. Composite pad brake unit vibration during train braking.

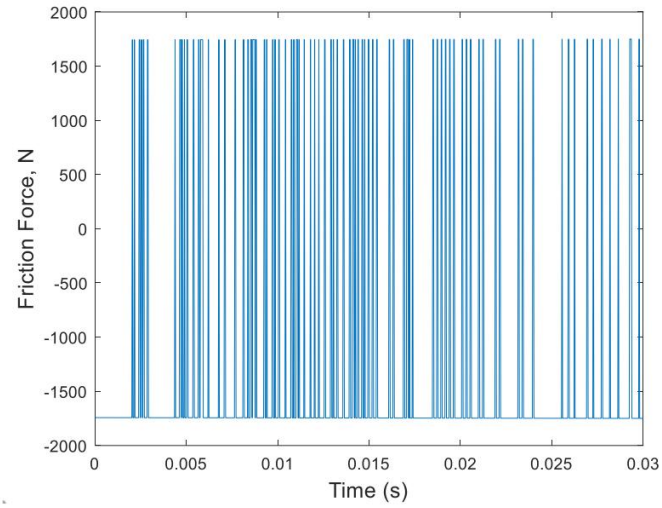

Figure 11. Changing friction force of cast iron pad brake unit during braking.

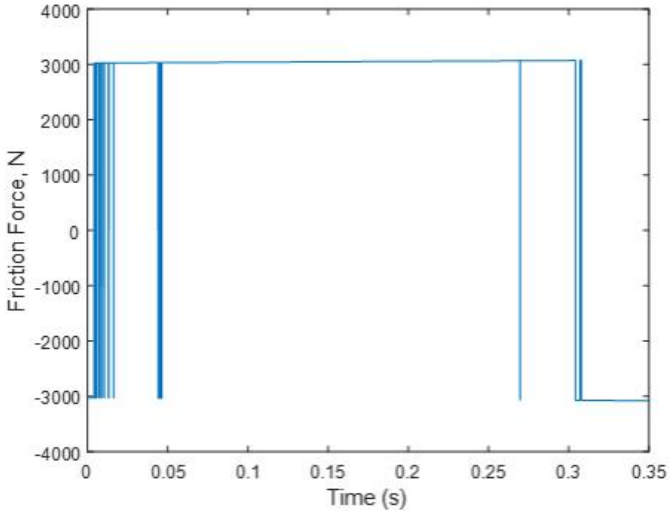

Figure 12. Changing friction force of composite pad brake unit during braking.

Figures 13 and **14** show the analyzed frequency-domain responses of the braking unit systems consisting of cast iron pads and composite pads. The system's primary oscillation frequencies were determined to be 0.3531 Hz and 0.3530 Hz, respectively. This suggests a marginal difference in the fundamental self-excited vibration frequencies between the composite and cast-iron brake unit systems. The observed low-frequency response reflects the global dynamic behavior of the brake unit governed by its mass–stiffness characteristics, rather than high-frequency squeal typically associated with stick–slip instability under intermittent adhesion.

This small discrepancy may be attributed to differences in material properties and frictional characteristics; however, given the extremely small numerical difference, it may also fall within the resolution of the numerical model. Therefore, the observed variation should be interpreted with caution and regarded as an indicative trend rather than a definitive material-dependent effect.

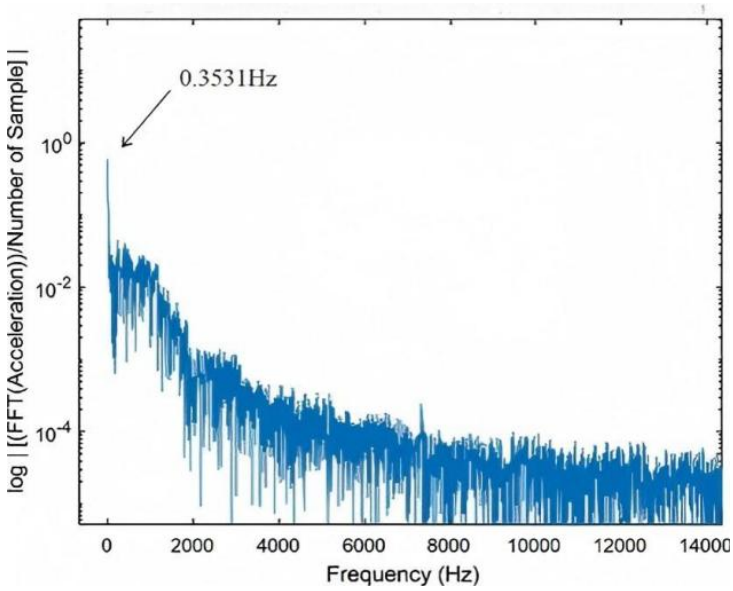

Figure 13. Single-sided amplitude spectrum of cast iron pad braking unit system.

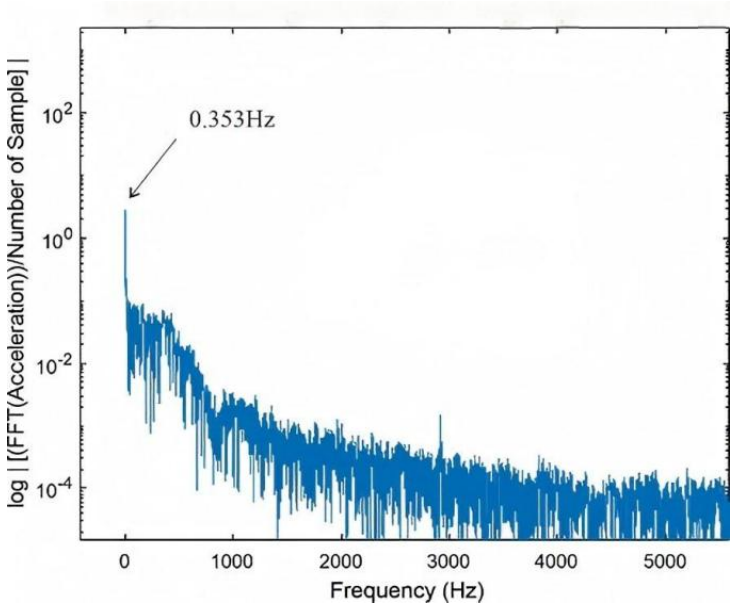

Figure 14. Single-sided amplitude spectrum of composite pad braking unit system.

7. Modal analysis of slack adjuster compensator

Following the identification of the dominant friction-induced vibration frequencies of the brake unit in Section 6, a modal analysis of the slack adjuster compensator is conducted to evaluate its natural frequencies and assess the potential for resonance. A commercial FE code ANSYS (ANSYS Inc., Canonsburg, PA, USA) was employed to simulate the response of the compensator. The brake tread was 3D-modeled as shown in **Figure 15**. The diameter and length of the tread of the brake were 30 mm and 290 mm, respectively.

Figure 15. 3-D model of the slack adjuster compensator.

7.1. Modeling, meshing, and boundary conditions for natural frequency analysis of compensator

The slack adjuster compensator model was generated by setting parameter values in the SolidWorks program. The resulting file was exported to ANSYS Workbench using the ".iges" file format. The ANSYS software, specifically the SOLID 187 module, was used to create a mesh for the 3D geometric model. The meshes were produced using the following parameters: mesh size for proximity and curvature, medium significance center, medium span angle center, and medium smoothing. **Figure 16** displays the finite element model of the brake tread, which is secured at

one end. One end of the compensator is fixed to represent its attachment to the brake rigging in the actual braking system.

Figure 16. Finite element model and boundary constraint of the compensator.

The compensator was assigned to be made of carbon steel AISI 1045. In modal analysis, Young's Modulus, Poisson's Ratio, and Mass Density were required inputs. Some of the material properties that were not used in the modal analysis are also reported for the benefit of the readers. These material properties are shown in **Table 6.**

Table 6. Mechanical properties of the slack adjuster compensator (AISI 1045).

Parameter	Unit	Value
Density	kg/m^3	7850
Young's Modulus	GPa	200
Tensile Yield Strength	MPa	589
Poisson Ratio		0.29

7.2. Model verification subsection

To ensure the validity of the FE model, mesh convergence and validation of the finite element model for the slack adjuster compensator were conducted first. The optimal mesh size was determined by a mesh convergence study, as shown in **Figure 17**, in which 0.003 m of mesh size was found to be adequate. There were 194,892 elements and 291,873 nodes in total.

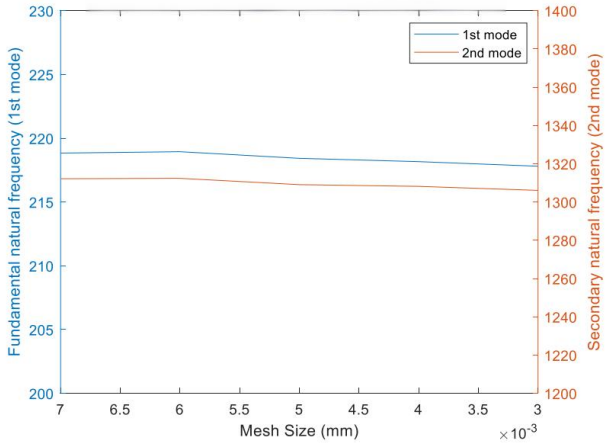

Figure 17. Mesh convergence study of finite element analysis with different mesh sizes with respect to fundamental and second natural frequencies of the slack adjuster compensator.

7.3. Results of FEA on slack adjuster compensator

Modal analysis of the slack adjuster compensator was conducted in ANSYS to simulate the free vibration response of the slack adjuster compensator. The output natural frequencies of slack adjuster compensator were obtained. The results of these simulations are shown in **Figures 18** and **19**. The first mode shape was of the fundamental natural frequency (216 Hz), and the second mode shape corresponding to the second natural frequency (1298.3 Hz). The identified natural frequencies (216.5 Hz and 1298.3 Hz) are several orders of magnitude higher than the dominant self-excited vibration frequency (~0.35 Hz) therefore indicating that resonance is unlikely under the investigated operating conditions.

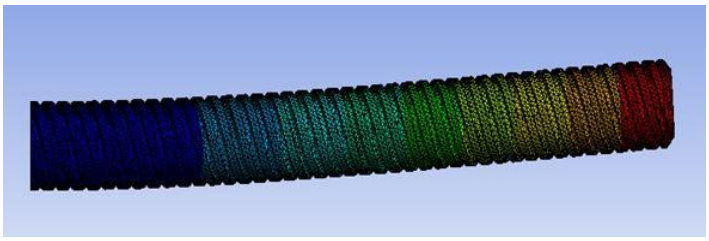

Figure 18. Mode 1 Natural Frequency 216.5 Hz.

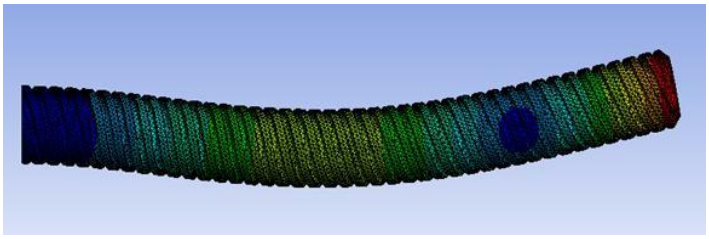

Figure 19. Mode 2 Natural Frequency 1298.3 Hz.

8. Discussion

The present study investigated friction-induced vibration in a tread brake system with particular emphasis on the interaction between the brake block and the slack adjuster compensator. The numerical results demonstrate that, under the investigated operating conditions, dry friction can give rise to self-excited vibration of the brake block during braking. However, the observed vibration response remains within a continuous sliding regime, and no classical stick–slip transition involving intermittent adhesion is identified.

The dominant vibration frequency extracted from the time- and frequency-domain analyses is approximately 0.35 Hz. This low-frequency response reflects the global dynamic behavior of the brake unit governed by its mass and stiffness characteristics, rather than high-frequency oscillations typically associated with stick– slip instability or brake squeal phenomena. The results therefore indicate that the friction-induced vibration observed in this study is fundamentally different in nature from classical stick–slip oscillations reported in the literature for other braking configurations.

A comparison between cast-iron and composite brake shoes reveals only a marginal difference in the dominant vibration frequency. This small discrepancy may be attributed to differences in material properties and the associated velocity-dependent

friction characteristics, within the limitations of the numerical model. Given the extremely small numerical difference between the frequencies obtained for the two materials, these results should be interpreted as indicative trends rather than as definitive material-dependent distinctions.

The modal analysis of the slack adjuster compensator further supports the interpretation of the vibration response. The natural frequencies of the compensator are found to be several orders of magnitude higher than the dominant self-excited vibration frequency of the brake unit. This large separation in frequency scales suggests that resonance between the friction-induced vibration of the brake block and the structural modes of the compensator is unlikely under the investigated operating conditions. Consequently, the vibration observed in the brake unit is not amplified by resonance effects associated with the compensator.

The present analysis is based on a simplified single-degree-of-freedom representation of the brake block and assumes continuous sliding at the contact interface. Effects such as temperature-dependent friction behavior, wear evolution, variations in contact conditions, and multi-degree-of-freedom coupling within the brake rigging are not considered. These factors may influence the vibration characteristics under different braking scenarios and operating conditions.

In addition, the modal analysis is performed on the slack adjuster compensator as an individual component with simplified boundary conditions. In practical applications, the dynamic characteristics of the assembled braking system may differ due to connection flexibility and system-level interactions. Future studies incorporating more detailed friction models, additional degrees of freedom, realistic boundary conditions, and experimental validation would be valuable for extending the applicability and robustness of the present findings.

9. Conclusion

This study investigated friction-induced vibration in a tread brake system with particular emphasis on the dynamic interaction between the brake block and the slack adjuster compensator. A simplified numerical model incorporating a velocity-dependent Coulomb friction formulation was developed to examine the vibration response of the brake block under representative braking conditions.

The numerical results indicate that dry friction can give rise to self-excited vibration of the brake block during braking. Under the investigated operating conditions, the contact interface remains in a continuous sliding regime, and no classical stick–slip transition involving intermittent adhesion is observed. The vibration response is therefore characterized as friction-induced self-excited vibration under sliding conditions.

Time- and frequency-domain analyses reveal a dominant low-frequency vibration component of approximately 0.35 Hz. This frequency reflects the global dynamic behavior of the brake unit governed by its mass and stiffness characteristics, rather than high-frequency oscillations typically associated with stick–slip instability or brake squeal phenomena. The results highlight the importance of considering system-level dynamics when interpreting vibration responses in tread brake systems.

A comparison between cast-iron and composite brake shoes shows only marginal differences in the dominant vibration frequency. Within the limitations of the numerical model, these differences suggest that the material-dependent friction characteristics have a limited influence on the global vibration frequency under the investigated conditions.

Modal analysis of the slack adjuster compensator demonstrates that its natural frequencies are several orders of magnitude higher than the dominant friction-induced vibration frequency of the brake unit. This large separation in frequency scales indicates that resonance between the brake block vibration and the compensator is unlikely under the operating conditions considered in this study.

The present analysis is subject to several limitations, including the use of a simplified single-degree-of-freedom brake block model and the assumption of continuous sliding at the contact interface. Effects such as temperature-dependent friction behavior, wear evolution, and multi-degree-of-freedom coupling within the brake rigging were not considered. Future work incorporating more detailed modeling approaches and experimental validation is recommended to further assess friction-induced vibration mechanisms in railway tread brake systems.

Author contributions: Conceptualization, NK and AS; methodology, NK; software, NK; validation, NK, and AS; formal analysis, NK; investigation, AS; resources, AS; data curation, NK; writing—original draft preparation, NK; writing—review and editing, AS; visualization, AS; supervision, AS; project administration, AS. Both authors have read and agreed to the published version of the manuscript.

Funding: This work was funded by Thailand Science Research and Innovation (TSRI), Thailand, through Program Management Unit for Competitiveness (PMUC), contract number C10F630261.

Institutional review board statement: Not applicable.

Informed consent statement: Not applicable.

Data availability statement: With this research, the results were obtained from many kinds of software such as ANSYS Workbench, SolidWorks, and MATLAB/Simulink simulations, and output files generated during the study are available from the corresponding author upon reasonable request.

Acknowledgment: We would like to acknowledge their contribution to the research including Kanit Industry Co., Ltd. and State Railway of Thailand (SRT) for their support of our research and these achievements.

Conflict of interest: The authors declare no conflict of interest.

References

1. Nguyen QS. Instability and friction. Comptes Rendus Mécanique. 2003; 331(1): 99–112.
2. Ibrahim RA. Friction-induced vibration, chatter, squeal, and chaos—Part II: dynamics and modeling. Applied Mechanics Reviews. 1994; 47(7): 227–253.
3. Ouyang H, Nack W, Yuan Y, et al. Numerical analysis of automotive disc brake squeal: A review. International

Journal of Vehicle Noise and Vibration. 2005; 1(3–4): 207–231.
4. Ehret M. Identification of a dynamic friction model for railway disc brakes. Proceedings of the Institution of Mechanical Engineers, Part F: Journal of Rail and Rapid Transit. 2021; 235(10): 1214–1224.
5. Meacci M, Allotta B, Rindi A, et al. A railway local degraded adhesion model including variable friction, energy dissipation and adhesion recovery. Vehicle System Dynamics. 2021; 59(11): 1697–1718.
6. Yang Z, Deng X, Li Z. Numerical modeling of dynamic frictional rolling contact with an explicit finite element method. Tribology International. 2019; 129: 214–231.
7. Yang Z, Deng X, Li Z, et al. An experimental study on the effects of friction modifiers on wheel–rail dynamic interactions with various angles of attack. Railway Engineering Science. 2022; 30(3): 360–382.
8. Ostermeyer GP, Wilkening L. Experimental investigations of the topography dynamics in brake pads. SAE International Journal of Passenger Cars–Mechanical Systems. 2013; 6(2013-01-2027): 1398–1407.
9. Lu C, Zhang Y, Liu Z, et al. Stick–slip characteristic analysis of high-speed train brake systems: A disc–block friction system with different friction radii. Vehicles. 2023; 5(1): 41–54.
10. Wang X, Wang J, Zhang Y, et al. Friction-induced stick-slip vibration and its experimental validation. Mechanical Systems and Signal Processing. 2020; 142: 106705.
11. Crowther AR, Singh R. Analytical investigation of stick-slip motions in coupled brake-driveline systems. Nonlinear Dynamics. 2007; 50(3): 463–481.
12. Crowther AR, Singh R. Identification and quantification of stick-slip induced brake groan events using experimental and analytical investigations. Noise Control Engineering Journal. 2008; 56(4): 235–255.
13. Zhang H, Qiao J, Zhang X. Nonlinear dynamics analysis of disc brake frictional vibration. Applied Sciences. 2022; 12(23): 12104.
14. Wei D, Zhang Y, Liu Z, et al. Bifurcation and chaotic behaviors of vehicle brake system under low speed braking condition. Journal of Vibration Engineering and Technologies. 2021; 9(8): 2107–2120.
15. Zhang Y, Liu Z, Stichel S. Study on the braking distance of composite brake blocks covered with ice for freight trains in winter. Proceedings of the Institution of Mechanical Engineers, Part F: Journal of Rail and Rapid Transit. 2023; 237(8): 1050–1059.
16. Günay M, Korkmaz ME, Özmen R. An investigation on braking systems used in railway vehicles. Engineering Science and Technology, an International Journal. 2020; 23(2): 421–431.
17. Mickoski H, Mickoski I, Zdraveski F. Investigation of self-excited vibrations in tread brake unit for railway vehicles. Journal of Vibroengineering. 2016; 18(6): 3881–3890.
18. Duan C, Singh R. Dynamics of a three-degree-of-freedom torsional system with a dry friction controlled path. Journal of Sound and Vibration. 2006; 289(4–5): 657–688.
19. Shin K, Brennan MJ, Oh J, et al. Analysis of disc brake noise using a two-degree-of-freedom model. Journal of Sound and Vibration. 2002; 254(5): 837–848.
20. Kalel N, Kulkarni M, Sharma A, et al. Suppression of brake noise and vibration using aramid and Zylon fibers: Experimental and numerical study. ACS Omega. 2022; 7(25): 21946–21960.
21. Dhanasekar M, Cole C, Handoko Y. Experimental evaluation of the effect of braking torque on bogie dynamics. International Journal of Heavy Vehicle Systems. 2007; 14(3): 308–330.
22. Sandoval-Valencia TE, Morales-Ibáñez A, Rivas-López JF, et al. Analysis of 3k experiments applied to railway braking: influence of contaminants and train speed. Vehicles. 2024; 6(4): 1886–1901.
23. Mickoski H, Djidrov M, Mickoski I. Estimation and analysis of various influential factors in the braking process of rail vehicles. Vehicle System Dynamics. 2021; 59(1): 1–16.
24. Fandom. General Electric GEA. Available online: https://thai-railway.fandom.com/wiki/General_Electric_(GEA) (accessed on 2 December 2025).
25. State Railway of Thailand. Diesel Locomotive. Available online: https://www.railway.co.th/More/Knowledge_Detail?value1=0049613716F4864B9ED01F76DB70384102000000E75BA90BDCBF851F48D7F685EAEBE880B4383FBFE196598EC58CC0B60D6FD888&value2=0049613716F4864B9ED01F76DB70384102000000DB0EEE2F59954C2B7CE998005E3448CEA66EC7051C6195CB2CACB3B0BA4CEBC6 (accessed on 2 December 2025). (in Thai)
26. Ivanov P, Petrov A, Dimitrov R, et al. Study of the influence of the brake shoe temperature and wheel tread on braking effectiveness. In: Proceedings of the International Scientific Conference Energy Management of Municipal Facilities and Sustainable Energy Technologies; 10–13 December 2019; Voronezh, Russia.
27. Abdo J, Abouelsoud AA. Analytical approach to estimate amplitude of stick-slip oscillations. Journal of Theoretical and Applied Mechanics. 2011; 49(4): 971–986.